

Self-Triggered Model Predictive Control for Perturbed Nonlinear Systems: An Iterative Implementation

Tao Wang¹, Pengfei Li¹, Yu Kang² and Yun-Bo Zhao¹

Abstract—In this paper, a novel iterative self-triggered model predictive control strategy is proposed for continuous-time nonlinear systems with external disturbances. For this strategy, the triggering instants are determined by iteratively using the self-triggered mechanism. To be specific, the triggering mechanism, on the one hand, determines the next sampling instants of the sensor by a prespecified condition, and, on the other hand, decides whether or not to treat the current sampling instant as the triggering instant. Without continuous monitoring of the state, the sensing cost of the sensor can be alleviated. The utilization of the sampling states after the triggering instant leads to a larger triggering interval, and the computational load of the controller can thus be reduced. The effectiveness of the proposed strategy is validated by a numerical example.

I. INTRODUCTION

The conventional execution of control tasks is usually implemented in a periodic way, which may cause unnecessary energy consumption, such as the unnecessary utilization of communication in networked control systems [1]. Therefore, it is desirable to reduce the number of transmissions. With this motivation, event-based control has given rise to much attention in recent years, since it offers the advantage of performing actuation only when the system needs attention [2]. Loosely speaking, event-triggered control and self-triggered control are two main event-based control approaches [3].

Model predictive control (MPC) has played an important role both in industry and academia for decades due to its conspicuous advantages in dealing with constraints and nonlinearities [4]. In a nonlinear MPC algorithm, a finite-time optimal control problem (OCP) needs to be solved repeatedly at every update time, resulting in a heavy computational load, which impedes the wide application of MPC. Therefore, it is quite necessary to design a scheduling strategy to reduce the consumption of computation resources when performing the MPC algorithm.

The event-based MPC framework provides a promising way to alleviate the computational load because it reduces the number of the OCP to be solved, see, e.g., [5]–[8] for

event-triggered MPC and [9]–[11] for self-triggered MPC. For event-triggered MPC, the OCP is solved only when some prescribed triggering conditions are violated. For example, the event-triggered MPC for continuous-time nonlinear systems is investigated in [5], where the computational load is reduced significantly. This result is extended in [6] by considering the state constraints. However, one may notice that continuous monitoring of the state is required for the event-triggered MPC of continuous-time systems, leading to high sensing cost. To overcome this drawback, intermittent sampling is proposed in [7], but the result is conservative because the sampling time is still relatively small (sampling frequency is high).

For self-triggered MPC, the OCP is solved and the next triggering time instant is determined according to the resultant predictive state and control sequences. As a result, the continuous monitoring is no longer required. However, for the perturbed system, since the predictive state error, i.e., a deviation between the predicted state and the actual one, is derived by using the worst case of the disturbance without resorting to the current system state, a conservative triggering instant may be obtained compared with the one obtained by the event-triggered strategy [12]. Therefore, although the sensing cost is reduced, the communication load may still heavy.

Motivated by the above facts, we propose an iterative self-triggered MPC strategy that combines both the advantages of the event- and self-triggered control. First, we determine the sampling instant in a self-triggered manner rather than periodically in event-triggered MPC. Then, the next sampling instant is obtained by employing the true predictive state error computed based on the sampled state. The sampling instant is set as a triggering instant only when the interval between the two consecutive sampling instants is rather small. The proposed strategy brings the following two benefits. (1) The self-triggered manner avoids continuous monitoring or periodic sampling, resulting in a lower sensing cost of the sensor than the one in [5], [6]. (2) Different from the conventional self-triggered MPC, the triggering instant is determined by using the true predictive state error at the sampling instants, leading to larger triggering intervals. Moreover, the triggering condition is adaptive to the triggering interval, which further enlarges the triggering interval compared with the results obtained by [5], [6].

This paper is organized as follows. Section II presents the system description and preliminaries. Section III gives the main results, including the design of the specific iterative self-triggered MPC strategy, and the feasibility and stability

*This work was supported by the National Key Research and Development Program of China (No. 2018AAA0100800, No. 2018YFE0106800), the National Natural Science Foundation of China (62103394, 62033012, 61725304 and 62173317), the Science and Technology Major Project of Anhui Province (912198698036), the Project funded by China Postdoctoral Science Foundation (2020M682036) (*Corresponding author: Yu Kang.*)

¹Tao Wang, Pengfei Li and Yun-Bo Zhao are with the Department of Automation, University of Science and Technology of China, Hefei, 230027, China wangtao@mail.ustc.edu.cn, {puffylee, ybzhao}@ustc.edu.cn

²Yu Kang is with the Department of Automation, State Key Laboratory of Fire Science and Institute of Advanced Technology, University of Science and Technology of China, Hefei, China. kangduyu@ustc.edu.cn

analysis. In Section IV, an illustrative example is shown to verified the effectiveness. Section V concludes this paper.

II. SYSTEM DESCRIPTION AND PRELIMINARIES

Consider the following continuous-time nonlinear system with additive disturbance

$$\dot{x}(t) = f(x(t), u(t)) + w(t), \quad t \geq t_0 \quad (1)$$

where $x(t) \in \mathcal{R}^n$ and $u(t) \in \mathcal{U} \subseteq \mathcal{R}^p$ denote the state and the control input, respectively, $w(t) \in \mathcal{W} = \{w \in \mathbb{R}^n : \|w\|_P \leq \rho, \rho > 0\}$ is the bounded disturbance with $\|w\|_P = \sqrt{w^T P w}$ and $P > 0$ being a positive definite matrix, and t_0 represents the initial time. \mathcal{U} is a compact set and contains the origin as an interior point. The function $f : \mathcal{R}^n \times \mathcal{U} \rightarrow \mathcal{R}^n$ is twice continuously differentiable satisfying $f(0, 0) = 0$, and is Lipschitz continuous in \mathcal{R}^n with a Lipschitz constant $L_f > 0$ depending on the weighted matrix P , i.e., $\forall x, y \in \mathcal{R}^n$, it holds that

$$\|f(x, u) - f(y, u)\|_P \leq L_f \|x - y\|_P. \quad (2)$$

The nominal system of the system (1) is obtained by letting $w(t) \equiv 0$,

$$\dot{\hat{x}}(t) = f(\hat{x}(t), \hat{u}(t)). \quad (3)$$

The linearization of the system in (1) around the origin is represented as

$$\dot{x}(t) = Ax(t) + Bu(t) + w(t) \quad (4)$$

where $A = \partial f / \partial x(0, 0)$ and $B = \partial f / \partial u(0, 0)$. For system (4), the following standard assumption is given.

Assumption 1 ([13]): For system (4), there exists a feedback control law $u(t) = Kx(t)$ such that $A_K = A + BK$ is Hurwitz.

Based on Assumption 1, the following lemma, which plays an important role in the feasibility and stability analysis, is given.

Lemma 1 ([5], [13]): Suppose that Assumption 1 holds. Given two positive definite matrices Q and R , there exists a positive definite matrix P , a constant $\varepsilon > 0$ and a feedback gain K , satisfying

$$\dot{V}(x(t))|_{\dot{x}(t)=f(x(t), Kx(t))} \leq -\|x(t)\|_{Q^*}^2 \quad (5)$$

and $Kx \in \mathcal{U}$ for all $x \in \Omega$, where $V(x) = \|x\|_P^2$, $\Omega = \{x \in \mathcal{R}^n : V(x) \leq \varepsilon^2\}$, and $Q^* = Q + K^T R K$.

III. MAIN RESULTS

In this section, the iterative self-triggered MPC strategy is designed, followed by the feasibility and stability analysis.

A. Iterative Self-Triggered MPC

The schematic block diagram of the iterative self-triggered MPC strategy is depicted in Fig.1 and the overview is stated as follows. The smart sensor consists of an iterative self-triggered mechanism (ISTM) and a sensor. The ISTM determines the sampling instants of the sensor on the one hand, and determines the transmission (triggering) instant of the sampled state on the other hand. If the triggering instant

is updated, the OCP is solved by the controller based on the current sampled state. Otherwise, the smart sensor continues to calculate the next sampling instant and checks whether or not to update the triggering instant.

In the following parts, we formulate the OCP, design the adaptive event-triggered condition, and based on which derive the ISTM.

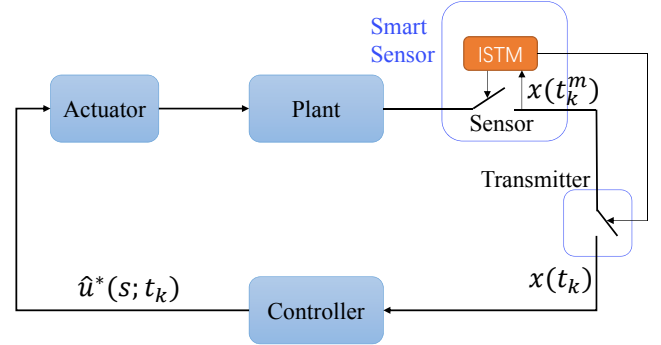


Fig. 1. The implementation of the iterative self-triggered MPC strategy

1) *OCP*: Denote by $t_k, k \in \mathbb{N}$ the triggering instants when the OCP is solved. The cost function is defined as:

$$J(\hat{x}(s; t_k), \hat{u}(s; t_k)) = \|\hat{x}(t_k + T; t_k)\|_P^2 + \int_{t_k}^{t_k + T} (\|\hat{x}(s; t_k)\|_Q^2 + \|\hat{u}(s; t_k)\|_R^2) ds, \quad (6)$$

where T is the prediction horizon. $\hat{u}(s; t_k)$ is the predicted control input trajectory and $\hat{x}(s; t_k)$ is the corresponding predicted state trajectory based on (3), where $s \in [t_k, t_k + T]$. Q, R and P are all positive weighted matrices. With the above descriptions, the OCP is then formulated as follows:

$$\min_{\hat{u}(s; t_k)} J(\hat{x}(s; t_k), \hat{u}(s; t_k))$$

$$\text{s.t. } \dot{\hat{x}}(s; t_k) = f(\hat{x}(s; t_k), \hat{u}(s; t_k)), \hat{x}(t_k; t_k) = x(t_k) \quad (7a)$$

$$\hat{u}(s; t_k) \in \mathcal{U} \quad (7b)$$

$$\hat{x}(t_k + T; t_k) \in \mathcal{X}_f, \quad (7c)$$

where $s \in [t_k, t_k + T]$, and $\mathcal{X}_f = \{x \in \mathcal{R}^n : \|x\|_P \leq \varepsilon_f^2\}$ is the terminal state constraint set with $0 < \varepsilon_f < \varepsilon$. The optimal control input $\hat{u}^*(\cdot; t_k)$ is generated by solving the above OCP, and the corresponding optimal state trajectory is denoted by $\hat{x}^*(\cdot; t_k)$. The optimal cost for the OCP at t_k is then denoted by $J^*(x(t_k)) = J(\hat{x}^*(s; t_k), \hat{u}^*(s; t_k))$.

2) *Adaptive event-triggered condition*: Since the predicted state trajectory is generated based on the nominal model (3), there is an error between the true and the nominal state, which may result in the infeasibility of the OCP if the triggering interval is too large. To tackle this issue, we design the following adaptive event-triggered condition to determine the triggering instants.

$$\|x(s) - \hat{x}^*(s; t_k)\|_P = (\varepsilon - \varepsilon_f) e^{-L_f(t_k + T - s)} \quad (8)$$

$$s - t_k = T$$

where $s > t_k$. Only when either of the above condition is satisfied, the event is triggered and the triggering instant is

updated to $t_{k+1} = s$. The OCP is solved again utilizing the state $x(t_{k+1})$ as the initial condition.

Observe that the above triggering condition depends on the current measurement $x(s; t_k)$, which requires continuous monitoring of the state, leading to high-cost sensing. Hence, this condition is not suitable for practical implementation.

Remark 1: Compared with the triggering conditions with a constant triggering threshold in [5], [6], the triggering threshold in condition (8) increases with respect to the triggering interval $(s - t_k)$, enjoying lower conservativeness.

3) *Self-triggered sampling:* The self-triggered mechanism is an effective way to avoid continuous monitoring, but large conservativeness will be brought because only the state at triggering instant and the upper bound of the disturbance are used. To overcome the shortcoming of the conventional self-triggered mechanism, we combine the ideas of the event- and self-triggered mechanism to propose the ISTM. The idea of the self-triggered sampling mechanism is depicted in Fig. 2. We iteratively employ the conventional self-triggered mechanism to determine the next sampling instant. One may notice that multiple samplings are included between two consecutive triggering instants. That is, the conservativeness is reduced compared with the conventional self-triggered mechanism via the utilization of the actual predicted state error and the increasing triggering threshold.

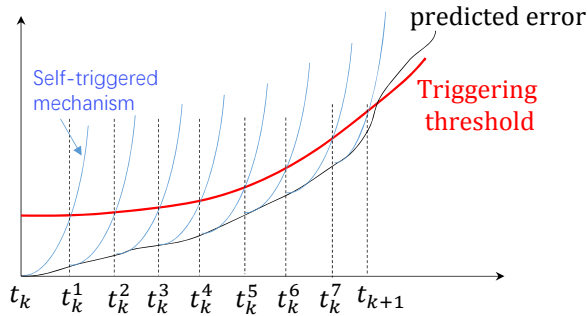


Fig. 2. Basic idea of self-triggered sampling mechanism

Now, we derive the iterative self-triggered condition inspired by (8) as follows. Let $t_k^m (k, m \in \mathbb{N})$ be the m th sampling instant after t_k and set $t_k^0 = t_k$. We design the following triggering condition that will be employed at each sampling instant.

$$\frac{\rho}{L_f} \left[e^{L_f(t_k + T - t_k^m)} - e^{L_f(t_k + T - t_k^{m+1})} \right] + \|x(t_k^m) - \hat{x}^*(t_k^m; t_k)\|_P e^{L_f(t_k + T - t_k^m)} = \varepsilon - \varepsilon_f. \quad (9)$$

As shown in Fig. 2, at each sampling instant t_k^m , the smart sensor samples the current state $x(t_k^m)$ to determine the next sampling instant t_k^{m+1} according to (9). If $t_k^{m+1} - t_k^m$ is lower than a prespecified constant σ , we set $t_{k+1} = t_k^m$ as the next triggering instant.

With the above descriptions, the next triggering instant t_{k+1} is determined as follows.

$$t_{k+1} = \begin{cases} t_k^m, & \text{if } t_k^{m+1} - t_k^m < \sigma \\ t_k + T, & \text{otherwise } t_k^{m+1} \geq t_k + T, \end{cases} \quad (10)$$

where $\sigma > 0$ is the minimum sampling interval.

The overall iterative self-triggered MPC strategy is demonstrated by Algorithm 1.

Algorithm 1: Iterative Self-Triggered MPC Algorithm

Initialization: Initial state $x(t_0)$; weighted matrices Q , R , and P ; parameters σ , ε , and ε_f ; prediction horizon T .

- 1: At any sampling instants $t_k^m, k \in \mathbb{N}$, the smart sensor samples the state $x(t_k^m)$ to determine the next sampling instant t_k^{m+1} via (9);
 - 2: If $t_k^{m+1} - t_k^m < \sigma$ or $t_k^{m+1} > t_k + T$, set $t_{k+1} = t_k^m$ or $t_{k+1} = t_k + T$ according to (10), $k = k + 1, m = 0$ and solve the OCP to obtain $\hat{u}^*(s; t_k)$;
 - 3: Apply $\hat{u}^*(s; t_k)$ to the system (1);
 - 4: Set $m = m + 1$ and go to step 1.
-

B. Feasibility Analysis

The feasibility means that the solution of the OCP in (7) exists at each triggering instant t_k , provided that the OCP admits a solution at t_0 . First, we give a lemma that formulates the upper bound of the state error between the actual state and the predicted one.

Lemma 2: If the nominal system (3) and the perturbed one (1) are controlled by the same control input $\hat{u}^*(s; t_k)$, then the state error between $x(s)$ and $\hat{x}^*(s; t_k)$ is bounded by

$$\|x(s) - \hat{x}^*(s; t_k)\|_P \leq \frac{\rho}{L_f} \left(e^{L_f(s - \bar{s})} - 1 \right) + \|x(\bar{s}) - \hat{x}^*(\bar{s}; t_k)\|_P e^{L_f(s - \bar{s})} \quad (11)$$

where $\bar{s} \geq t_k$.

Proof: From (1) and (3), we obtain

$$\begin{aligned} & \|x(s) - \hat{x}^*(s; t_k)\|_P \\ &= \|x(\bar{s}) + \int_{\bar{s}}^s f(x(\tau), \hat{u}^*(\tau; t_k)) + w(\tau) d\tau \\ & \quad - \hat{x}^*(\bar{s}; t_k) - \int_{\bar{s}}^s f(x(\hat{x}^*(\tau; t_k), \hat{u}^*(\tau; t_k)) d\tau\|_P \\ & \leq \|x(\bar{s}) - \hat{x}^*(\bar{s}; t_k)\|_P + \rho(s - \bar{s}) \\ & \quad + \int_{\bar{s}}^s L_f \|x(\tau) - \hat{x}^*(\tau; t_k)\|_P d\tau. \end{aligned}$$

Using the Gronwall-Bellman inequality yields

$$\begin{aligned} & \|x(s) - \hat{x}^*(s; t_k)\|_P \\ & \leq \frac{\rho}{L_f} \left(e^{L_f(s - \bar{s})} - 1 \right) + \|x(\bar{s}) - \hat{x}^*(\bar{s}; t_k)\|_P e^{L_f(s - \bar{s})}. \end{aligned}$$

This proof is completed. \blacksquare

Based on Lemma 2, we can obtain a lower bound of the triggering interval, which is stated in the following lemma.

Lemma 3: For the system (1), if the triggering instants sequence $t_k, k \in \mathbb{N}$ are generated by Algorithm 1 and the prediction horizon is chosen such that

$$T \geq \frac{1}{L_f} \ln \frac{L_f(\varepsilon - \varepsilon_f)}{\rho} \quad (12)$$

is fulfilled then the triggering interval is lower bounded by δ , that is, $\inf_{k \in \mathbb{N}} \{t_{k+1} - t_k\} \geq \delta$, where $\delta := \frac{1}{L_f} \ln \frac{\rho e^{L_f T}}{\rho e^{L_f T} - L_f(\varepsilon - \varepsilon_f)}$.

Proof: According to (10), the first sampling instant t_k^1 after t_k may be the latest triggering instant. In other words, $t_{k+1} \geq t_k^1$ always holds. Substituting $t_k^0 = t_k$ into (9), we have

$$\frac{\rho}{L_f} (e^{L_f T} - e^{L_f(t_k + T - t_k^1)}) \leq \varepsilon - \varepsilon_f.$$

Using the condition in (12), we have

$$t_{k+1} - t_k \geq t_k^1 - t_k \geq \frac{1}{L_f} \ln \frac{\rho e^{L_f T}}{\rho e^{L_f T} - L_f(\varepsilon - \varepsilon_f)}.$$

This completes the proof. \blacksquare

The recursive feasibility is shown by the induction principle, therefore, the initial feasibility is assumed at first. Recall that the definition of the feasible set in [14] is $\mathcal{X} = \{x(t_0) \in \mathcal{R}^n\}$: the OCP admits a solution for a given T

Assumption 2 ([5]): The prediction horizon is chosen such that $\mathcal{X} \neq \emptyset$ and $x(t_0) \in \mathcal{X}$.

Theorem 1: Consider the system (1) with Assumptions 1 and 2. Algorithm 1 is recursively feasible if the minimum triggering interval satisfies

$$\delta \geq \frac{\bar{\lambda}(P)}{\underline{\lambda}(Q^*)} \ln \frac{\varepsilon^2}{\varepsilon_f^2} \quad (13)$$

where $\bar{\lambda}(P)$ is the maximum eigenvalue of P and $\underline{\lambda}(Q^*)$ is the minimum eigenvalue of Q^* .

Proof: First, we construct a feasible solution candidate at t_{k+1} based on the optimal solution $\hat{u}^*(s; t_k)$ at t_k as:

$$\tilde{u}(s; t_{k+1}) = \begin{cases} \hat{u}^*(s; t_k), & s \in [t_k, t_k + T], \\ K\tilde{x}(s; t_{k+1}), & s \in [t_k + T, t_{k+1} + T] \end{cases} \quad (14)$$

where the state trajectory $\tilde{x}(s; t_{k+1}), s \in [t_{k+1}, t_{k+1} + T]$ is subject to the nominal system dynamics (3) with $\tilde{x}(t_{k+1}; t_{k+1}) = x(t_{k+1})$. In the remainder of this proof, we need to show that $\tilde{u}(s; t_{k+1})$ is a feasible solution for the OCP at t_{k+1} , which is equivalent to proving that the control input constraint in (7b) and the terminal state constraint and (7c) are satisfied.

To begin with, we show that the following inequality holds based on the condition in (9)

$$\|x(t_{k+1}) - \hat{x}^*(t_{k+1}; t_k)\|_P \leq (\varepsilon - \varepsilon_f) e^{-L_f(t_k + T - t_{k+1})} \quad (15)$$

From Lemma 2, we have

$$\|x(t_{k+1}) - \hat{x}^*(t_{k+1}; t_k)\|_P \leq \frac{\rho}{L_f} \left(e^{L_f(t_{k+1} - t_k^m)} - 1 \right) + \|x(t_k^m) - \hat{x}^*(t_k^m; t_k)\|_P e^{L_f(t_{k+1} - t_k^m)}. \quad (16)$$

By virtue of (9) and the fact that $t_{k+1} \leq t_k^{m+1}$, we obtain

$$\|x(t_k^m) - \hat{x}^*(t_k^m; t_k)\|_P e^{L_f(t_{k+1} - t_k^m)} + \frac{\rho}{L_f} \left(e^{L_f(t_{k+1} - t_k^m)} - 1 \right) \leq (\varepsilon - \varepsilon_f) e^{-L_f(t_k + T - t_{k+1})}. \quad (17)$$

Combining (16) and (17), we obtain (15).

In the sequel, the satisfaction of the constraints is proved.

- $\tilde{x}(s; t_{k+1}) \in \mathcal{X}_f$: The core of proving the satisfaction of the terminal state constraint is to derive the upper bound of the error between $\tilde{x}(s; t_{k+1})$ and $\hat{x}^*(s; t_k)$ for $s \in [t_{k+1}, t_k + T]$. First, due to the same control input $\hat{u}^*(s; t_k)$ being applied during $s \in [t_k, t_k + T]$, we obtain

$$\begin{aligned} & \|\tilde{x}(s; t_{k+1}) - \hat{x}^*(s; t_k)\|_P \\ &= \|\tilde{x}(t_{k+1}; t_{k+1}) + \int_{t_{k+1}}^s f(\tilde{x}(\tau; t_{k+1}), \tilde{u}(\tau; t_{k+1})) d\tau \\ & \quad - \hat{x}^*(t_{k+1}; t_k) - \int_{t_{k+1}}^s f(\hat{x}^*(\tau; t_k), \hat{u}^*(\tau; t_k)) d\tau\|_P \\ &\leq \|\tilde{x}(t_{k+1}; t_{k+1}) - \hat{x}^*(t_{k+1}; t_k)\|_P \\ & \quad + \int_{t_{k+1}}^s L_f \|\tilde{x}(\tau; t_{k+1}) - \hat{x}^*(\tau; t_k)\|_P \\ &\leq \|x(t_{k+1}) - \hat{x}^*(t_{k+1}; t_k)\|_P e^{L_f(s - t_{k+1})} \end{aligned} \quad (18)$$

where the triangle inequality and the Gronwall-Bellman inequality are used. By virtue of (15), we obtain $\|x(t_{k+1}) - \hat{x}^*(t_{k+1}; t_k)\|_P = (\varepsilon - \varepsilon_f) e^{-L_f(t_k + T - t_{k+1})}$. Then, substituting $s = t_k + T$ into (18), one can obtain

$$\|\tilde{x}(t_k + T; t_{k+1}) - \hat{x}^*(t_k + T; t_k)\|_P \leq \varepsilon - \varepsilon_f. \quad (19)$$

Since $\hat{x}^*(t_k + T; t_k) \in \mathcal{X}_f$, one obtains $\|\tilde{x}(t_k + T; t_{k+1})\|_P \leq \varepsilon$. In this case, the state-feedback Kx is used. Recalling Lemma 1, we have $\dot{V}(\tilde{x}(s; t_{k+1})) \leq -\|\tilde{x}(s; t_{k+1})\|_{Q^*} \leq -\underline{\lambda}(Q^*)/\bar{\lambda}(P) V(\tilde{x}(s; t_{k+1}))$. Utilizing the comparison principle [15], we obtain

$$V(\tilde{x}(s; t_{k+1})) \leq \varepsilon^2 e^{-\frac{\underline{\lambda}(Q^*)}{\bar{\lambda}(P)}(s - t_k - T)}. \quad (20)$$

Thus, we have $\|\tilde{x}(s; t_{k+1})\|_P \leq \varepsilon, \forall s \in [t_k + T, t_{k+1} + T]$. Substituting $s = t_{k+1} + T$ into (20) results in $V(\tilde{x}(t_{k+1} + T; t_{k+1})) \leq \varepsilon^2 e^{-\underline{\lambda}(Q^*)/\bar{\lambda}(P)(t_{k+1} - t_k)} \leq \varepsilon^2 e^{-\underline{\lambda}(Q^*)/\bar{\lambda}(P)\delta}$. Considering the condition in (13), one can obtain $V(\tilde{x}(t_{k+1} + T; t_{k+1})) \leq \varepsilon_f^2$, i.e., $\tilde{x}(t_{k+1} + T; t_{k+1}) \in \mathcal{X}_f$.

- $\tilde{u}(s; t_{k+1}) \in \mathcal{U}$: For $s \in [t_{k+1}, t_k + T]$, $\tilde{u}(s; t_{k+1}) = \hat{u}^*(s; t_k) \in \mathcal{U}$. For $s \in [t_k + T, t_{k+1} + T]$, $\tilde{u}(s; t_{k+1}) = K\tilde{x}(s; t_{k+1})$. Then, $\tilde{u}(s; t_{k+1}) \in \mathcal{U}, \forall s \in [t_k + T, t_{k+1} + T]$ follows from Lemma 1.

This completes the proof. \blacksquare

C. Stability analysis

In this section, the stability of the closed-loop system under the implementation of Algorithm 1 is analyzed. Specifically, we will prove the closed-loop system is regional Input-to-State practically Stable (ISpS) [16].

Theorem 2: Suppose that Assumptions 1 and 2 hold, the conditions in (12) and (13) are fulfilled. Then, the closed-loop system is ISpS in \mathcal{X} under Algorithm 1.

Proof: According to [16, Definition 4], one should prove that the system allows a ISpS-Lyapunov function in \mathcal{X} . First, we set $V(x(t)) = J(\tilde{x}(s; t), \tilde{u}(s; t))$ as the Lyapunov function candidate. In particular, if $t = t_k$, we

set $V(x(t_k)) = J(\hat{x}^*(s; t_k), \hat{u}^*(s; t_k))$. In what follows, we show that $V(x(t))$ is an ISpS-Lyapunov function, that is, the following hold

$$\alpha_1(\|x(t)\|) \leq V(x(t)) \leq \alpha_2(\|x(t)\|) \quad (21)$$

$$\dot{V}(x(t)) \leq -\alpha_3(\|x(t)\|) + \beta(\rho) + c \quad (22)$$

for all $x(s; t) \in \mathcal{X}$, $t \in [t_k, t_k + T]$, where α_1, α_2 and α_3 are three \mathcal{K}_∞ functions, β is a \mathcal{K} function and $c > 0$ is a constant.

We first consider $t = t_k$. The lower bound of $V(x(t_k))$ can be easily obtained and is omitted here. From Lemma 1, integrating inequality (5) from t_k to $t_k + T$ yields

$$\begin{aligned} & \|\hat{x}^*(t_k + T; t_k)\|_P^2 - \|\hat{x}^*(t_k; t_k)\|_P^2 \\ & \leq - \int_{t_k}^{t_k+T} (\|\hat{x}^*(\tau; t_k)\|_Q^2 + \|\hat{u}^*(\tau; t_k)\|_R^2) d\tau. \end{aligned} \quad (23)$$

Substituting (23) into (6) yields $V(x(t_k)) \leq \|\hat{x}^*(t_k; t_k)\|_P^2 \leq \bar{\lambda}(P)\|x(t_k)\|^2 \triangleq \bar{\alpha}_2(\|x(t_k)\|)$ for all $x(t_k) \in \Omega$. Then, we follow the similar idea in [16, Lemma 4] to obtain the upper bound of $V(x(t_k))$ in \mathcal{X} . There exist a \bar{V} such that $V(x(t_k)) \leq \bar{V}, \forall x(t_k) \in \mathcal{X}$. Define a set $B_r = \{x \in \mathcal{R}^n : \|x\| \leq r\} \subset \mathcal{X}_f$. Let $\theta = \max(1, \frac{\bar{V}}{\alpha_2(r)})$, one can obtain $V(x(t_k)) \leq \alpha_2(\|x(t_k)\|)$ where $\alpha_2(\|x\|) = \theta \bar{\alpha}_2(\|x\|)$.

It remains to show that (22) holds. The derivative of the Lyapunov function candidate is defined as

$$\dot{V}(x(t_k)) \triangleq \lim_{h \rightarrow 0^+} \frac{V(x(t_k + h)) - V(x(t_k))}{h}. \quad (24)$$

Denote the difference of the cost function between two time instants t_k and $t_k + h$ by $\Delta V(x(t_k)) = V(x(t_k + h)) - V(x(t_k))$, then we have (25) below.

$$\begin{aligned} \Delta V(x(t_k)) &= - \underbrace{\int_{t_k}^{t_k+h} (\|\hat{x}^*(\tau; t_k)\|_Q^2 + \|\hat{u}^*(\tau; t_k)\|_R^2) d\tau}_{\Delta_1} \\ &+ \underbrace{\int_{t_k+h}^{t_k+T} (\|\tilde{x}(\tau; t_k + h)\|_Q^2 - \|\hat{x}^*(\tau; t_k)\|_Q^2) d\tau}_{\Delta_2} \\ &+ \underbrace{\int_{t_k+T}^{t_k+h+T} (\|\tilde{x}(\tau; t_k + h)\|_Q^2 + \|\tilde{u}(\tau; t_k + h)\|_R^2) d\tau}_{\Delta_3} \\ &+ \underbrace{\|\tilde{x}(t_k + h + T; t_k + h)\|_P^2 - \|\hat{x}^*(t_k + T; t_k)\|_P^2}_{\Delta_3}. \end{aligned} \quad (25)$$

In the sequel, we consider Δ_1, Δ_2 , and Δ_3 one by one.

$$\Delta_1 \leq -\underline{\lambda}(Q) \int_{t_k}^{t_k+h} \|\hat{x}^*(\tau; t_k)\|^2 d\tau. \quad (26)$$

Define constants L_Q and L_P such that $\|x\|_Q^2 - \|y\|_Q^2 \leq L_Q\|x - y\|_Q, \forall x, y \in \mathcal{X}$ and $\|x\|_P^2 - \|y\|_P^2 \leq L_P\|x - y\|_P, \forall x, y \in \Omega$. Then, combining (8), (13) and (18), Δ_2 becomes

$$\Delta_2 \leq \int_{t_k+h}^{t_k+T} L_Q(\|\tilde{x}(\tau; t_k + h) - \hat{x}^*(\tau; t_k)\|_Q) d\tau$$

$$\begin{aligned} & \leq \frac{\bar{\lambda}(\sqrt{Q})}{\underline{\lambda}(\sqrt{P})} \int_{t_k+h}^{t_k+T} L_Q(\|\tilde{x}(\tau; t_k + h) - \hat{x}^*(\tau; t_k)\|_P) d\tau \\ & \leq \frac{\bar{\lambda}(\sqrt{Q})}{\underline{\lambda}(\sqrt{P})} \int_{t_k+h}^{t_k+T} L_Q\|x(t_k + h) - \hat{x}^*(t_k + h; t_k)\|_P \\ & \quad \times e^{L_f(s-t_k-h)} d\tau \\ & \leq \frac{\bar{\lambda}(\sqrt{Q})L_Q\rho}{\underline{\lambda}(\sqrt{P})L_f^2} (e^{L_f h} - 1) (e^{L_f(T-h)} - 1). \end{aligned} \quad (27)$$

By virtue of Lemma 1 and (19), it follows

$$\begin{aligned} \Delta_3 &= \int_{t_k+T}^{t_k+h+T} \|\tilde{x}(\tau; t_k + h)\|_{Q^*}^2 d\tau \\ &+ \|\tilde{x}(t_k + h + T; t_k + h)\|_P^2 - \|\hat{x}^*(t_k + T; t_k)\|_P^2 \\ &\leq \|\tilde{x}(t_k + T; t_k + h)\|_P^2 - \|\hat{x}^*(t_k + T; t_k)\|_P^2 \\ &\leq L_P (e^{L_f h} - 1) e^{L_f(T-h)}. \end{aligned} \quad (28)$$

Substituting (26), (27) and (28) into (25) and considering $h \rightarrow 0^+$, we can obtain

$$\dot{V}(x(t_k)) \leq -\alpha_3(\|x(t_k)\|) + \beta(\rho) + c \quad (29)$$

where $\alpha_3(\|x(t_k)\|) = \underline{\lambda}(Q)\|x(t_k)\|^2$, $\beta(\rho) = \frac{\bar{\lambda}(\sqrt{Q})L_Q}{\underline{\lambda}(\sqrt{P})L_f} (e^{L_f T} - 1) \rho$, and $c = L_P L_f e^{L_f T}$.

When $t \in (t_k, t_k + T]$, (21) and (22) can be obtained by using the same proof line as above, which are omitted in this paper due to the page limit. The proof is completed. ■

IV. NUMERICAL EXAMPLE

This section validates the effectiveness of the proposed iterative self-triggered MPC strategy by an example.

Consider a cart-spring-damper system [5] and its system dynamics are formulated as

$$\begin{cases} \dot{x}_1(t) = x_2(t) \\ \dot{x}_2(t) = -\frac{k}{m} e^{-x_1(t)} x_1(t) - \frac{h}{m} x_2(t) + \frac{u(t)}{m} + \frac{w(t)}{m} \end{cases} \quad (30)$$

where the component x_1 and x_2 are the displacement and the velocity of cart, respectively. The mass of the cart is $m = 1.25\text{kg}$, the stiffness of the nonlinear spring is $k = 0.9\text{N/m}$, and the viscous damping is $h = 0.42\text{N.s/m}$. $u(t)$ is the control input, and $w(t)$ is the disturbance. The control input constraint is set as $\mathcal{U} = \{u_i : -1 \leq u \leq 1\}$. The upper bound of the disturbance is $\rho = 0.001$. The initial state is $x(t_0) = (0.2, -0.2)$.

To implement Algorithm 1, we set the matrix $Q = \begin{bmatrix} 0.5 & 0 \\ 0 & 0.5 \end{bmatrix}$, $R = 0.1$. Using LQR to obtain the feed-back gains $K = [-1.5104, -2.5721]$. The matrix P is calculated as $P = \begin{bmatrix} 1.2551 & -0.6151 \\ -0.6151 & 0.8054 \end{bmatrix}$, and the level set and the terminal set are determined as $\varepsilon = 0.2, \varepsilon_f = 0.18$ by utilizing the method in [13]. Thus, the Lipschitz constant is $L_f = 2.5$. The minimum sampling interval is $\sigma = 0.05\text{s}$. The prediction horizon is set as $T = 3\text{s}$ according to Lemma 3 and Theorem 1.

The displacement, velocity, and control input of the cart under Algorithm 1 are shown in Figs. 3-4, respectively. It can be seen that the control input constraint is satisfied and the

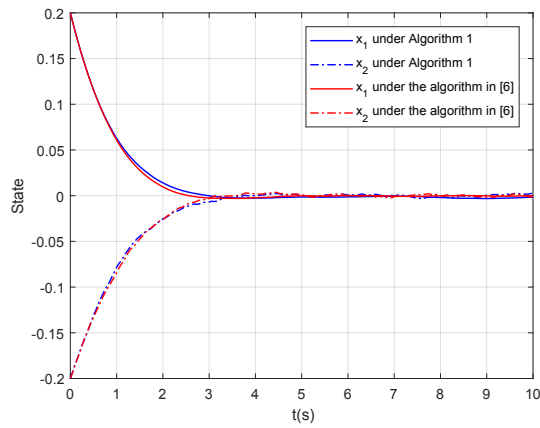


Fig. 3. The displacement and velocity of the cart.

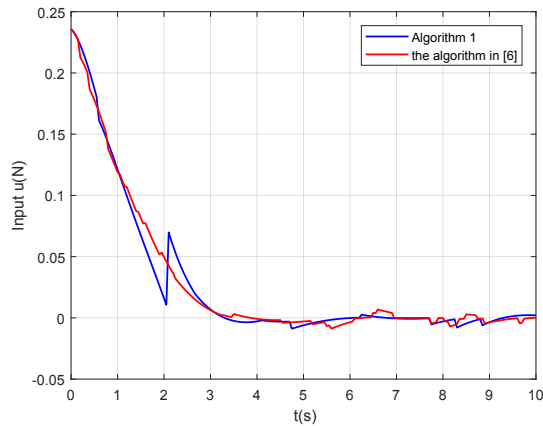


Fig. 4. The control input of the cart.

closed-loop system is ISpS. The triggering instants and the sampling instants are illustrated in Fig. 5. It can be observed that the sampling behaviour is taken place only at certain sampling instants instead of periodically. Additionally, the triggering interval is greater than $\delta = 0.45$ according to Lemma 3, and the computational load is reduced significantly compared to the algorithm in [6].

V. CONCLUSION

In this paper, the self-triggered MPC for continuous-time nonlinear systems with external disturbance has been investigated, and a novel iterative self-triggered MPC strategy is proposed. With this strategy, the sensing cost has been alleviated efficiently by avoiding continuous monitoring of the state, and the computational load has been reduced by an adaptive triggering condition. The feasibility of the proposed strategy and stability of the system have been proved. The effectiveness of the proposed strategy has been validated by a simulation example.

REFERENCES

[1] A. Eqtami, D. V. Dimarogonas, and K. J. Kyriakopoulos, "Novel event-triggered strategies for model predictive controllers," in *Proc. 50th IEEE Conf. Decision Control & Eur. Control Conf.*, 2011, pp. 3392–3397.

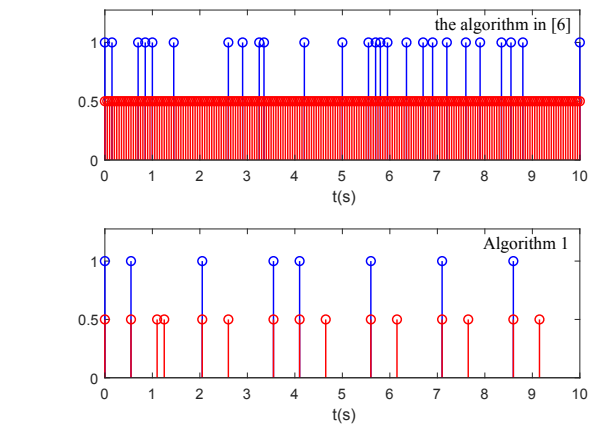


Fig. 5. The triggering instants (black line) and the sampling instants (red line).

[2] W. Heemels, K. H. Johansson, and P. Tabuada, "An introduction to event-triggered and self-triggered control," in *51st IEEE Conference on Decision and Control*, 2012, pp. 3270–3285.

[3] Y. Wang, W. X. Zheng, and H. Zhang, "Dynamic event-based control of nonlinear stochastic systems," *IEEE Transactions on Automatic Control*, vol. 62, no. 12, pp. 6544–6551, 2017.

[4] J. B. Rawlings, D. Q. Mayne, and M. Diehl, *Model predictive control: theory, computation, and design*, 2nd ed. Nob Hill Publishing Madison, WI, 2017.

[5] H. Li and Y. Shi, "Event-triggered robust model predictive control of continuous-time nonlinear systems," *Automatica*, vol. 50, no. 5, pp. 1507–1513, 2014.

[6] C. Liu, J. Gao, H. Li, and D. Xu, "Aperiodic robust model predictive control for constrained continuous-time nonlinear systems: An event-triggered approach," *IEEE Transactions on Cybernetics*, vol. 48, no. 5, pp. 1397–1405, 2017.

[7] K. Hashimoto, S. Adachi, and D. V. Dimarogonas, "Event-triggered intermittent sampling for nonlinear model predictive control," *Automatica*, vol. 81, pp. 148–155, 2017.

[8] P. Li, T. Wang, Y. Kang, and Y.-B. Zhao, "Event-triggered adaptive horizon model predictive control for perturbed nonlinear systems," in *59th IEEE Conference on Decision and Control*, 2020, pp. 2392–2397.

[9] A. Eqtami, S. Heshmati-Alamdari, D. V. Dimarogonas, and K. J. Kyriakopoulos, "Self-triggered model predictive control for nonholonomic systems," in *2013 European Control Conference*, 2013, pp. 638–643.

[10] P. Li, Y. Kang, Y.-B. Zhao, and T. Wang, "A novel self-triggered MPC scheme for constrained input-affine nonlinear systems," *IEEE Transactions on Circuits and Systems II: Express Briefs*, vol. 68, no. 1, pp. 306–310, 2020.

[11] Z. Sun, L. Dai, K. Liu, D. V. Dimarogonas, and Y. Xia, "Robust self-triggered MPC with adaptive prediction horizon for perturbed nonlinear systems," *IEEE Trans. Autom. Control*, vol. 64, no. 11, pp. 4780–4787, Nov. 2019.

[12] M. Kishida, M. Kögel, and R. Findeisen, "Event-triggered actuator signal update using self-triggered sampled data for uncertain linear systems," in *2017 American Control Conference*, 2017, pp. 3035–3041.

[13] H. Chen and F. Allgöwer, "A quasi-infinite horizon nonlinear model predictive control scheme with guaranteed stability," *Automatica*, vol. 34, no. 10, pp. 1205–1217, 1998.

[14] D. Q. Mayne, J. B. Rawlings, C. V. Rao, and P. O. Scokaert, "Constrained model predictive control: Stability and optimality," *Automatica*, vol. 36, no. 6, pp. 789–814, 2000.

[15] H. K. Khalil and J. W. Grizzle, *Nonlinear systems*, 3rd ed. Prentice hall Upper Saddle River, NJ, 2002.

[16] M. Rubagotti, D. M. Raimondo, A. Ferrara, and L. Magni, "Robust model predictive control with integral sliding mode in continuous-time sampled-data nonlinear systems," *IEEE Transactions on Automatic Control*, vol. 56, no. 3, pp. 556–570, 2010.